Mechanical Properties of Hybrid Composites using Finite Element Method Based Micromechanics

S. BANERJEE AND B. V. SANKAR

ABSTRACT

A micromechanical analysis of the unit cell of a unidirectional hybrid composite is performed using finite element method. The fibers are assumed to be circular and packed in a hexagonal array. The effects of volume fractions of the two different fibers used and also their relative locations within the unit cell are studied. The failure envelopes of the hybrid composites are developed from the micro-stresses within the unit cell for various macro-stress states using the Direct Micromechanics Method (DMM). From the DMM results various phenomenological failure criteria such as maximum stress, maximum strain and Tsai-Hill theories are developed for the hybrid composites. The results for hybrid composites are compared with single fiber composites.

Sayan Banerjee, Graduate Student (sbanerjee@ufl.edu)
B. V. Sankar, Ebaugh Professor (sankar@ufl.edu)
Department of Mechanical and Aerospace Engineering, PO Box 116250, University of Florida, Gainesville, FL 32611, USA

INTRODUCTION

Hybrid composites contain more than one type of fiber in a single matrix material. In principle, several different fiber types may be incorporated into a hybrid, but it is more likely that a combination of only two types of fibers would be most beneficial [1]. They have been developed as a logical sequel to conventional composites containing one fiber. Hybrid composites have unique features that can be used to meet various design requirements in a more economical way than conventional composites. This is because expensive fibers like graphite and boron can be partially replaced by less expensive fibers such as glass and Kevlar [2]. Some of the specific advantages of hybrid composites over conventional composites include balanced strength and stiffness, balanced bending and membrane mechanical properties, balanced thermal distortion stability, reduced weight and/or cost, improved fatigue resistance, reduced notch sensitivity, improved fracture toughness and/or crack arresting properties, and improved impact resistance [1].

Experimental techniques can be employed to understand the effects of various fibers, their volume fractions and matrix properties in hybrid composites. These experiments require fabrication of various composites with the above mentioned parameters, which are time consuming and cost prohibitive. Therefore, a computational model is created as will be described in detail later, which might be easily altered to model hybrid composites of different volume fractions of constituents, hence saving the designer valuable time and resource.

The mechanical properties of hybrid short fiber composites can be evaluated using the rule of hybrid mixtures (RoHM) equation, which is widely used to predict the strength and modulus of hybrid composites [3]. It is shown however, that RoHM works best for longitudinal modulus and longitudinal tensile strength of the hybrid composites. Since, modulus values in a composite are volume averaged over the constituent microstresses, the overall modulus of the composite has little correlation with the randomness of the fiber location. Strength values on the other hand are not primarily functions of strength of the constituents; they are however dependent on the fiber/matrix interaction and interface quality. In tensile test, any minor (microscopic) imperfection on the specimen may lead to stress build-up and failure could not be predicted directly by RoHM equations [4].

The computational model presented in this paper takes into account, random fiber location inside a representative volume element for every volume fraction ratio of fibers, in this case, carbon and glass. The effect of randomization seems to have considerable effect on the transverse strength of the hybrid composites. As for the transverse modulus, a semi empirical relation similar to Halpin-Tsai equations has been derived, with the Halpin-Tsai parameter obtained for hexagonal packing of circular fibers. Finite element based micromechanics is used to obtain the results, which show a good match with experimental results for effective modulus for hybrid composites with ternary systems (two fibers and a matrix) [5]. Direct Micromechanics Method (DMM) is used for predicting strength, which is based on first element failure method; although conservative, it provides a good estimate for failure initiation.

MODEL FOR HYBRID COMPOSITE

In most composites the fiber packing arrangement is statistically random in nature, so that the properties are same in any direction perpendicular to the fiber (i.e. properties along the 2-direction are same as that along the 3-direction, see Fig 3), and the material can be considered transversely isotropic [6]. For this paper, the fibers are assumed to be arranged in a hexagonal arrangement in an epoxy matrix, since such an arrangement can most accurately represent transverse isotropy. We assume a representative volume element (RVE) consisting of 50 fibers embedded in an epoxy matrix. Multiple numbers of fiber were selected to allow randomization of fiber locations. Hybrid composites are created by varying the number of carbon and glass fibers to obtain composites of various volume fractions.

As a practical example the hybrid composite of polypropylene matrix reinforced with short glass and carbon fibers is shown in Fig 1 [7]. The black circles represent glass fibers (V_{fg}=6.25%) and the white circles represent carbon fibers (V_{fc}=18.75%). In order to represent such a random arrangement, we consider multiple fibers as mentioned before, and the arrangement is as shown in Fig 2. Green and red represent glass and carbon fibers, respectively, while the matrix is shown in white. The rectangular RVE is assumed to repeat itself in the 2-3-plane. Also, it is assumed that the radii of the fibers are equal and only the number of carbon and glass fibers within the RVE was varied to change the volume fractions. This gives us much more flexibility in creating the finite element mesh.

Although, this RVE is very simplistic and entails some basic assumptions such as constant fiber diameter, fixed fiber location and absence of voids, it will be still useful in understanding the effect of varying the fiber volume fractions on the mechanical properties. Since, the actual composite extends through the page in the longitudinal direction, a plane strain analysis is sufficient in this case. A combined fiber volume fraction of 60% (V_{fg}+ V_{fc}=0.6) is assumed for all the composites analyzed in this paper. The proportions of the reinforcements have been varied to obtain five different hybrid composites. The volume fractions of glass and carbon fibers were determined as follows:

$$V_{fg} = \left(\frac{N_g}{N_T}\right) * \ 0.6$$
$$V_{fc} = 0.6 - V_{fg}$$

where, N_g = Number of fibers of glass

N_T = Total number of fibers (50 in the present example)

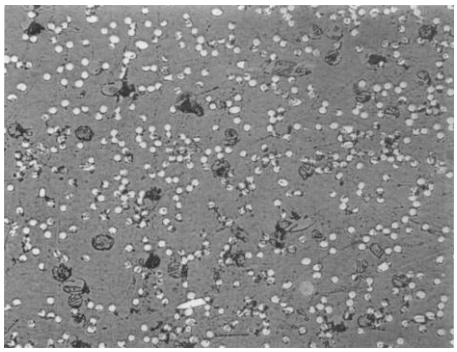

Fig 1. Central area of a hybrid composite with V_f (carbon) = 18.75% and V_f (glass) = 6.25%

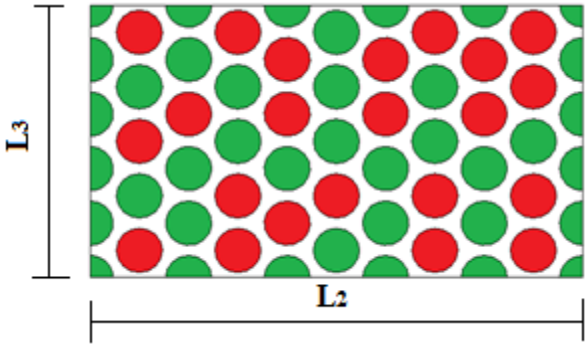

Fig 2. A representative volume element (RVE) for the hybrid composite

MICROMECHANICAL ANALYSIS

The RVE of the hybrid composite was analyzed using the finite element method. It is assumed that a uniform macrostress exists through the composite. It is also assumed that the fibers are circular in cross section an arranged hexagonally across the representative volume element (RVE) which has a square boundary. The composite is assumed to be under a state of uniform strain at the macroscopic level called macroscale strains or macrostrains, and the corresponding stresses are called macrostresses. However, the microstresses, which are the actual stresses in the constituent phases in the RVE will have spatial variation. The macrostresses are average stresses required to produce a given state of macro-deformations, and they can be computed from the finite element results. The macrostresses and macrostrains follow the following constitutive relation:

$$\{\sigma^M\} = [C]\,\{\varepsilon^M\}$$

where, $[C]$ is the stiffness matrix of the homogenized composite.. In performing the micromechanical analysis, the Ris subjected to six independent macrostrains. For each applied non-zero macrostrain, it is also subjected to periodic boundary conditions such that all other macrostrains are zero. The six cases are [8]: Case 1: ε_{11}^M = 1; Case 2: ε_{22}^M = 1; Case 3: ε_{33}^M = 1; Case 4: γ_{12}^M = 1; Case 5: γ_{13}^M = 1; Case 6: γ_{23}^M = 1.

Finite Element Analysis

For cases 1, 2 and 4, three- and four-node plane strain elements, CPE3/CPE4 in the commercial finite element program Abaqus, were used. For Case 3, generalized plane strain elements CPEG3/CPEG4 were used. Cases 5 and 6 involve out of plane shear deformations and plane strain elements cannot be used for this purpose. Shear deformable plate elements were used for the two longitudinal shear cases. The plate was assumed to have infinite bending and extensional stiffness so that the transverse shear was the only active deformation mechanism in the plate. The periodic boundary conditions (PBC) maintain equal boundary displacements with the adjacent unit cells to satisfy the compatibility of displacements on opposite faces of the unit cells and also enforce the continuity of stresses [9]. The unit cell is thus subjected to various macrostrains using the PBC described in Table 1. For each strain case, microstresses were calculated in each element in the finite element model and volume averaged to find the six macrostresses. This populates one column of the *C* matrix. This process is repeated for all the six strain cases. The finite element model, which contains 27,000 elements, is shown in Fig 3. In the above finite element model, the opposite faces of the unit cell should have corresponding nodes for enforcing the periodic boundary conditions using multi-point constraints [8]. The *C* matrix thus obtained can be inverted to obtain the compliance matrix or *S* matrix, from which the elastic constants can be computed using the following relations:

$$\begin{pmatrix} \sigma_1 \\ \sigma_2 \\ \sigma_3 \\ \tau_{23} \\ \tau_{13} \\ \tau_{12} \end{pmatrix} = \begin{bmatrix} C_{11} & C_{12} & C_{13} & 0 & 0 & 0 \\ C_{21} & C_{22} & C_{23} & 0 & 0 & 0 \\ C_{31} & C_{32} & C_{33} & 0 & 0 & 0 \\ 0 & 0 & 0 & C_{44} & 0 & 0 \\ 0 & 0 & 0 & 0 & C_{55} & 0 \\ 0 & 0 & 0 & 0 & 0 & C_{66} \end{bmatrix} \begin{pmatrix} \varepsilon_1 \\ \varepsilon_2 \\ \varepsilon_3 \\ \gamma_{23} \\ \gamma_{13} \\ \gamma_{12} \end{pmatrix}$$

$$[C]^{-1} = [S] = \begin{bmatrix} \frac{1}{E_1} & \frac{-\nu_{12}}{E_1} & \frac{-\nu_{13}}{E_1} & 0 & 0 & 0 \\ \frac{-\nu_{21}}{E_2} & \frac{1}{E_2} & \frac{-\nu_{23}}{E_2} & 0 & 0 & 0 \\ \frac{-\nu_{31}}{E_3} & \frac{-\nu_{32}}{E_3} & \frac{1}{E_3} & 0 & 0 & 0 \\ 0 & 0 & 0 & \frac{1}{G_{23}} & 0 & 0 \\ 0 & 0 & 0 & 0 & \frac{1}{G_{13}} & 0 \\ 0 & 0 & 0 & 0 & 0 & \frac{1}{G_{12}} \end{bmatrix}$$

TABLE 1. Periodic Boundary Conditions for rectangular RVE
(L_2 and L_3 being the dimensions of the RVE along 2 & 3 directions, respectively)

	Constraint between Left and Right faces	**Constraint between Top and Bottom faces**	**Out of Plane Strains**
$\varepsilon_{11} = 1$	$u_i(L_2, x_3) - u_i(0, x_3) = 0$ i =2,3	$u_i(x_2, L_3) - u_i(x_2, 0) = 0$ i =2,3	ε_{11}=1, γ_{12}=0, γ_{13}=0
$\varepsilon_{22} = 1$	$u_2(L_2, x_3) - u_2(0, x_3) = L_2$ $u_3(L_2, x_3) - u_3(0, x_3) = 0$	$u_i(x_2, L_3) - u_i(x_2, 0) = 0$ i =2,3	ε_{11}=1, γ_{12}=0, γ_{13}=0
$\varepsilon_{33} = 1$	$u_i(L_2, x_3) - u_i(0, x_3) = 0$ i =2,3	$u_2(x_2, L_3) - u_2(x_2, 0) = 0$ $u_3(x_2, L_3) - u_3(x_2, 0) = L_3$	ε_{11}=1, γ_{12}=0, γ_{13}=0
γ_{12}=1	$u_3(L_2, x_3) - u_3(0, x_3) = L_2$	$u_3(x_2, L_3) - u_3(x_2, 0) = 0$	ε_{11}=0, γ_{13}=0
γ_{13}=1	$u_3(L_2, x_3) - u_3(0, x_3) = 0$	$u_3(x_2, L_3) - u_3(x_2, 0) = L_3$	ε_{11}=0, γ_{12}=0
γ_{23}=1	$u_2(L_2, x_3) - u_2(0, x_3) = 0$ $u_3(L_2, x_3) - u_3(0, x_3) = L_2/2$	$u_2(x_2, L_3) - u_2(x_2, 0) = L_3/2$ $u_3(x_2, L_3) - u_3(x_2, 0) = 0$	ε_{11}=0, γ_{12} =0, γ_{13}=0

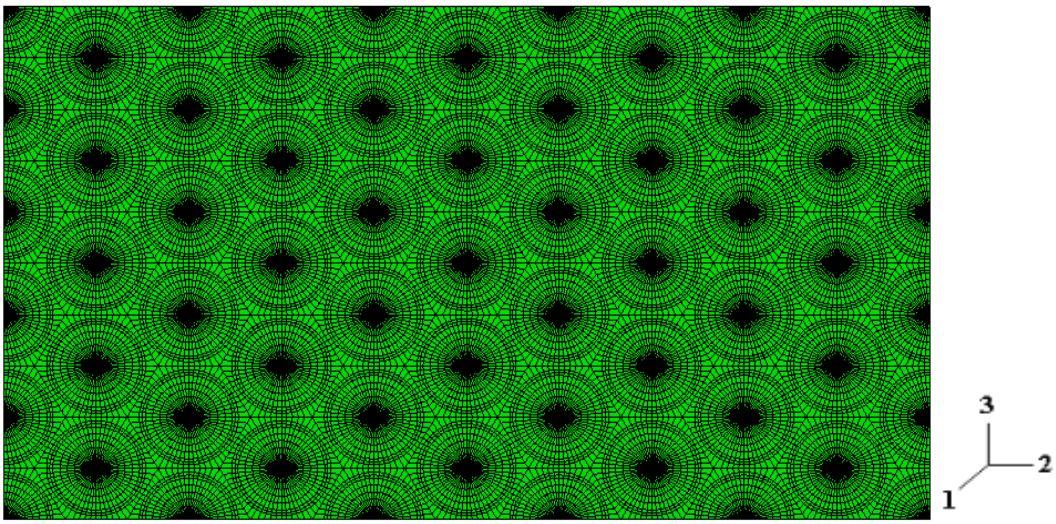

Fig 3. Finite element model of the RVE

The material properties (elastic moduli) for the various constituents are as per Table 2. For a composite to have transversely isotropic behavior in the 2-3-plane, it has to follow the relation:

$$G_{23} = \frac{E_2}{2(1 + \nu_{23})}$$

As shown in Table 3, all the composites for the present analysis closely possess transverse isotropy. One reason for such a behavior may be attributed to the hexagonal packing of the fiber, which represents better isotropy in the 2-3 plane. As for the hybrid composites, 10 samples of each volume fraction ratio were

considered. The mean values for the elastic constants were used to study the effect of hybridization on the elastic constants.

Rule of mixtures was also used to predict the longitudinal modulus E_1 for carbon-epoxy and glass-epoxy composite. However for the hybrid composites, the rule of mixtures was modified in order to accommodate the volume fraction of both carbon and glass fibers, and it is shown later that the E_1 for hybrid composites obtained as such, matches well with the results from finite element analysis.

For the transverse modulus, E_2, and for shear modulus G_{12}, semi-empirical formulations similar to Halpin-Tsai equation was derived. For hybrid composites, Halpin-Tsai equation was modified to accommodate volume fraction of both the fibers. Once again, the results show a good match with those from finite element analysis. The results obtained from both the finite element analyses as well as from empirical formulations are tabulated in Table 4. The variations of the moduli with volume fraction of the hybrid composites are also shown.

EVALUATION OF STRENGTH PROPERTIES

Failure is predicted using the Direct Micro-Mechanics (DMM), in which every element in the finite element model is checked for failure. A flowchart that describes DMM is shown in Fig 4. Thus for a given state of macrostress, we need to determine the microstresses in every element in the fiber and the matrix phases. The macrostrain for a given state of macrostress can be obtained from the constitutive relations using the modulus values obtained for that composite using the following relation:

$$\{\varepsilon^M\} = [C^{-1}]\{\sigma^M\}$$

From the unit cell analysis as discussed before, we already have the microstresses in every element for six independent unit macrostrain cases. Thus, the microstresses for a given macrostress state can be obtained using the principle of superposition as follows:

$$\{\sigma^{(e)}\} = [F^{(e)}]\{\varepsilon^M\}$$

where $\{\sigma^{(e)}\}$ is the microstress in Element e, and the matrix $[F^{(e)}]$ represents the microstresses in Element e for various states of unit microstrains. For example, the first column in F_{iI} contains the six microstresses in Element e caused by unit macrostrain ε_{11}^M. In the present work it is assumed that there exist no thermal residual stresses in the composite [8].

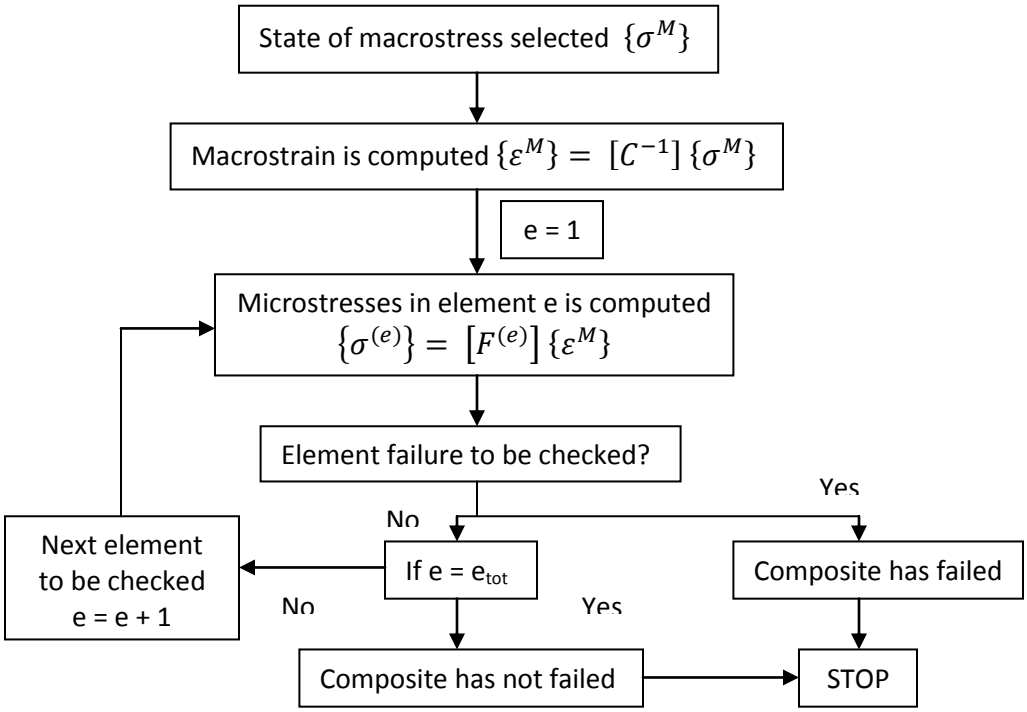

Fig 4. Flow chart for Direct Micromechanics method for failure

In order to determine if an element has failed or not, we need failure criteria for fiber and matrix materials. It is assumed, that failure criteria for fibers and matrix phases are known. We have considered a quadratic interaction failure criteria for carbon fiber and maximum normal stress failure criteria for glass fiber and epoxy. The quadratic failure criterion closely resembles the one proposed by Hashin for unidirectional fiber composites [10]. As mentioned before, literally all unidirectional fiber composites are transversely isotropic in the 2-3 plane, since the fiber arrangement is statistically random. Further, as stresses in 2-3 plane are invariant of the rotation around the longitudinal axis, failure criterion must be invariant of any rotation around 1 axis. Hence, it can be safely assumed that fiber failure in the longitudinal direction is controlled by σ_1 only. Also, since σ_2, σ_3 and τ_{23} form a state of plane stress and 2-3 plane being an isotropic plane, it can be assumed that there exists two principal stresses which should control the failure in the 2-3 plane. Also, because of transverse isotropy, τ_{12} and τ_{13} should be approximately equal. Hence, the resultant of the axial shear stresses can be critical if it reaches the shear strength of carbon.

For glass fiber and epoxy matrix we have used maximum principal stress criterion for predicting failure. Also, in the present paper, we have assumed that the composite has failed even if only one element in the fiber or matrix fails. Although this assumption is very conservative, it gives as a good estimate of initial failure of the composite [8]. Similarly, for the hybrid composites, depending on the type of element, carbon, glass or matrix, we have to apply respective criterion for failure as described above. Using such methods, we have generated failure envelopes for the composite in various stress spaces.

RESULTS AND DISCUSSIONS

Carbon and glass were chosen as the two fiber materials, and an epoxy as the matrix material. Further comparison has also been made with empirical formulation whenever possible.

TABLE 2. Elastic properties of various constituents

Property	E-glass fiber [9]	Carbon fiber (IM7) [11]	Epoxy [9]
E_1 (GPa)	72.4	263	3.5
E_2, E_3 (GPa)	72.4	19	3.5
G_{12}, G_{13} (GPa)	30.2	27.6	1.29
G_{23} (GPa)	30.2	7.04	1.29
ν_{12}, ν_{13}	0.2	0.2	0.35
ν_{23}	0.2	0.35	0.35

Elastic Constants

As shown in Fig. 5, longitudinal modulus, E_1 for the hybrid composites vary linearly with volume fraction of the constituents. E_1 for Carbon/Epoxy being the highest and then linearly decreases as volume fraction of carbon reduces from 0.6 to 0. The comparison of E_1 with results from standard models like the rule of mixtures was also done. It shows that the RoHM do a good job in predicting the longitudinal modulus and the poisson's ratios, ν_{12} and ν_{13}. It is important to note here, that for the three phase composites, the rule of mixtures should incorporate volume fraction of all three constituents

$$E_1 = E_{1c}V_{fc} + E_{1g}V_{fg} + E_mV_m$$

This formulation captures the hybridization effect on longitudinal modulus and poisson's ratios very successfully as shown in Fig 5 and Fig 7.

A general method to estimate the properties E_2 and G_{12} involves the use of semi-empirical equations that are adjusted to match experimental results such as the Halpin-Tsai equation. For the transverse modulus, the Halpin-Tsai equation is:

$$\frac{E_2}{E_m} = \frac{1 + \xi\eta V_f}{1 - \eta V_f}$$

where,

$$\eta = \frac{\left(\frac{E_f}{E_m}\right) - 1}{\left(\frac{E_f}{E_m}\right) + \xi}$$

and ξ is a curve-fitting parameter, which is dependent on the fiber packing arrangement. The corresponding equation for G_{12} is obtained by replacing Young's moduli E_2, E_f and E_m in the above equation by shear moduli G_{12}, G_f and G_m respectively. Halpin and Tsai found that the value $\xi = 2$ gave an excellent fit to the finite difference elasticity solution of Adams and Doner [12] for the transverse modulus of a square array of circular fibers. For the same material and fiber volume fraction, a value of $\xi = 1$ gave excellent agreement for G_{12} [13].

But for circular fibers in a hexagonal array, we don't have an explicit value for ξ. In this paper, we have used the finite element solution for E_2 and G_{12} for Carbon/Epoxy and Glass/Epoxy composites, to iteratively find the value for ξ. This resulted in $\xi = 1.14$ for transverse modulus E_2 and $\xi = 1.01$ for G_{12}. We propose the following empirical formula for E_2 of hybrid composites:

$$\frac{E_2}{E_m} = \frac{1 + \xi(\eta_c V_{fc} + \eta_g V_{fg})}{1 - (\eta_c V_{fc} + \eta_g V_{fg})}$$

where,

$$\eta_c = \frac{\left(\frac{E_{fc}}{E_m}\right) - 1}{\left(\frac{E_{fc}}{E_m}\right) + \xi}$$

$$\eta_g = \frac{\left(\frac{E_{fg}}{E_m}\right) - 1}{\left(\frac{E_{fg}}{E_m}\right) + \xi}$$

For the hybrid composite we use $\xi = 1.14$ for transverse modulus E_2 and $\xi = 1.01$ for G_{12}. The variation of E_2 and G_{12} with volume fraction of carbon is shown in Fig 6 and Fig 8, respectively. One can note that the finite element results match the modified Halpin-Tsai equations for hybrid composites very well. Tabulated below are the summary of the results for elastic properties for all the composites, followed by the plots showing effects of hybridization on the various elastic moduli. The moduli are plotted with respect to volume fraction of carbon fiber as it increases from left to right i.e. from glass/epoxy to carbon/epoxy composite.

Table 3. Comparison of G_{23} to test transverse isotropy. A ratio of $G_{23} / G'_{23} = 1$ denotes perfect tramnsvese isotropy

	Volume of Reinforcement		G_{23}	$G'_{23} = \frac{E_2}{2(1+\nu_{23})}$	G_{23} / G'_{23}
	Carbon	**Glass**			
Carbon/Epoxy	0.6	0	3.04	3.05	0.997
	0.54	0.06	3.14	3.15	0.997
	0.42	0.18	3.36	3.37	0.997
Hybrid	0.3	0.3	3.6	3.62	0.994
	0.18	0.42	3.88	3.90	0.995
	0.06	0.54	4.19	4.20	0.998
Glass/Epoxy	0	0.6	4.35	4.37	0.995

Table 4. Comparision of results from finite element method and Halpin-Tsai relations

Composite	E_2			G_{12}		
	FEA (GPa)	Halpin-Tsai (GPa)	% Diff	FEA (GPa)	Halpin-Tsai (GPa)	% Diff
Carbon/epoxy	8.77	8.59	2.07	4.41	4.41	-0.05
	9.05	8.88	1.84	4.41	4.42	-0.04
	9.66	9.52	1.47	4.43	4.43	-0.04
Hybrid	10.33	10.22	1.08	4.44	4.44	0.00
	11.05	11.00	0.50	4.45	4.45	-0.06
	11.82	11.86	-0.37	4.46	4.46	-0.06
Glass/epoxy	12.21	12.33	-1.02	4.47	4.47	0.05

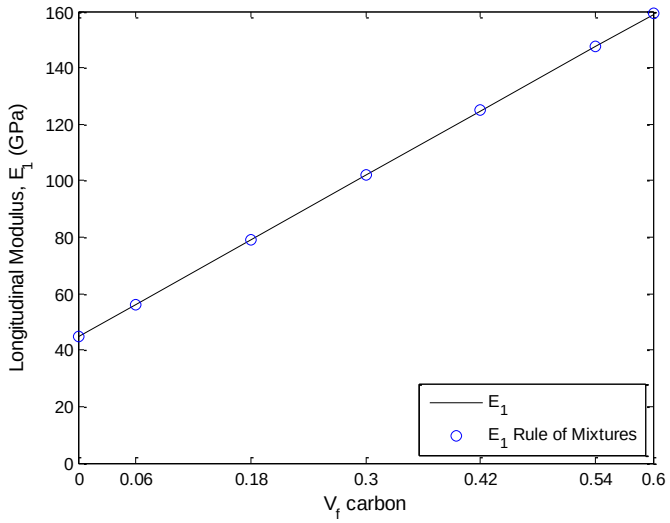

Fig 5. Effect of Hybridization on E_1

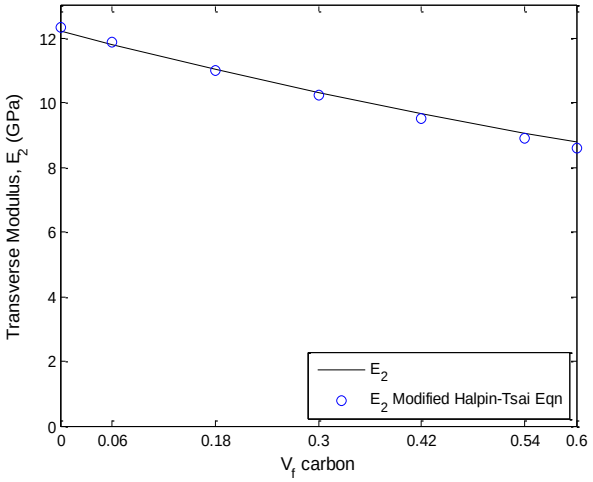

Fig 6. Effect of hybridization on E_2

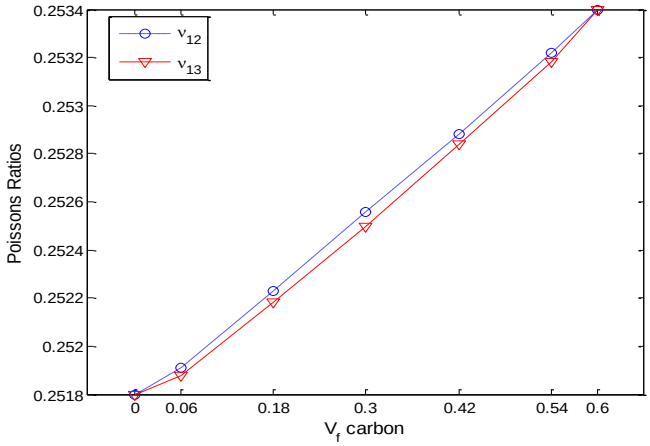

Fig 7. Effect of hybridization on Poisson's Ratios

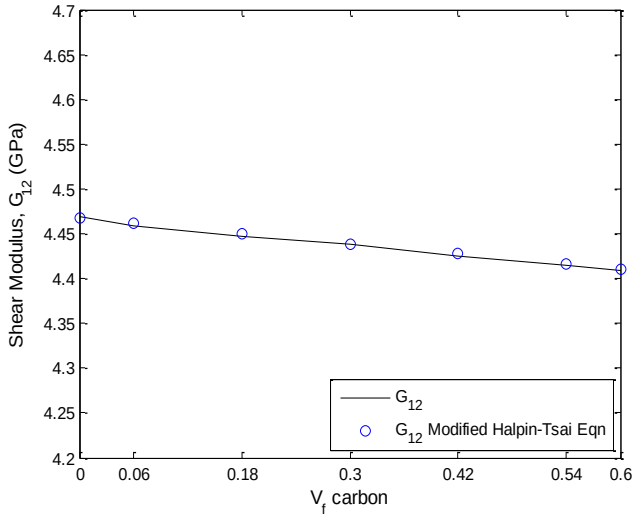

Fig 8. Effect of hybridization on G_{12}

Strength Properties

Composite failure can generally be defined by either fiber failure or matrix failure, considering the interface has infinite strength and doesn't fail. The fiber failure strain can be defined by $e_{f1}^{(+)} = s_{f1}^{(+)}/E_{f1}$ and the matrix failure strain would be $e_{m1}^{(+)} = s_{m1}^{(+)}/E_{m1}$, where $s_{f1}^{(+)}$, E_{f1}, $s_{m1}^{(+)}$, E_{m1} would be longitudinal tensile strength of fiber, fiber longitudinal modulus, longitudinal tensile strength of matrix and matrix longitudinal modulus respectively. In this case, since $e_{f1}^{(+)}$ is higher than $e_{m1}^{(+)}$, we can conclude that matrix will govern the failure. So, if matrix failure is the criterion, composite failure will occur at the strain level corresponding to the matrix failure strain, $e_{m1}^{(+)}$. Hence, when the stress in the matrix reaches the matrix tensile strength, $s_{m1}^{(+)}$, the fiber stress reaches the value $s_{fm1}^{(+)} = E_{f1}e_{m1}^{(+)}$, the composite stress reaches the composite strength, $s_L^{(+)}$, which is given by the following equation [6]:

$$s_L^{(+)} = s_{fm1}^{(+)}V_f + s_{m1}^{(+)}(1 - V_f)$$

This equation gives a good measure of the failure strength for initiation of failure. The results from finite element analysis clearly show a close match with the value from the above equation. The empirical relation for longitudinal tensile strength can be modified for hybrid composites, by including the volume fractions for both the reinforcements as follows:

$$s_L^{(+)} = s_{fm1c}^{(+)}V_{fc} + s_{fm1g}^{(+)}V_{fg} + s_{m1}^{(+)}(1 - V_f)$$

where, $s_{fm1c}^{(+)} = E_{f1c}e_{m1}^{(+)}$

$$s_{fm1g}^{(+)} = E_{f1g}e_{m1}^{(+)}$$

and $V_f = V_{fc} + V_{fg}$

Empirical relation for prediction of transverse moduli has not been developed yet. Table 5A and 5B lists the strength properties for the constituents used in this analysis, whereas Table 6 summarizes the strength properties for carbon/epoxy and glass/epoxy composites. While dealing with compressive strength, tensile strengths are replaced by compressive strengths and no buckling effect was studied here.

Table 5A. Strength properties of unidirectional fibers [9]

	Carbon	**Glass**
Longitudinal Tensile Strengths (MPa)	4120	1104
Longitudinal Compressive Strength (MPa)	2990	1104
Transverse Tensile and Compressive Strengths (MPa)	298	1104
Shear Strength (MPa)	1760	460

Table 5B. Strength properties for matrix [9]

	Epoxy
Tensile Strength (MPa)	49
Compressive Strength (MPa)	121
Shear Strength (MPa)	93

Table 6. Summary of Strength properties for Composites

Strength	Carbon/Epoxy			Glass/Epoxy		
	FEA	Empirical	% Diff	FEA	Empirical	% Diff
Longitudinal Tensile Strength (MPa)	2,130	2,230	4.50	598	628	4.76
Longitudinal Compressive Strength (MPa)	1807	1811	0.23	683	511	-33.82
Transverse Tensile Strength (MPa)	41	47	12.19	38	46	15.91
Transverse Compressive Strength (MPa)	101	115	12.19	86	113	23.78

Table 7. Comparison of Longitudinal Tensile strength for composites with empirical results

Composite	V_{fc}	V_{fg}	FEA (MPa)	Empirical (MPa)	% Diff
Carbon/epoxy	0.6	0	2130	2229	4.43
	0.54	0.06	1972	2069	4.67
	0.42	0.18	1665	1748	4.77
Hybrid	0.3	0.3	1360	1428	4.78
	0.18	0.42	1055	1108	4.79
	0.06	0.54	750	788	4.81
Glass/Epoxy	0	0.6	598	628	4.74

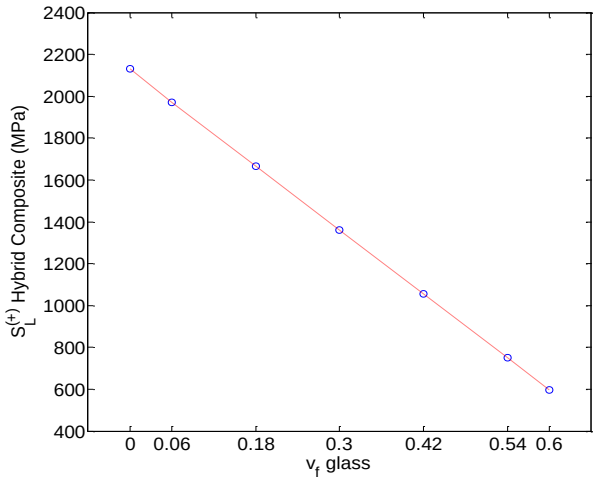

Fig 9. Variation of longitudinal tensile strength with volume fraction of reinforcement

Table 7 shows a good match between the rule and mixtures predictions and those obtained from finite element method, for the Longitudinal Tensile strength for hybrids. Failure envelopes were constructed by applying bi-axial macrostress to the different composites. The envelopes thus obtained are compared with existing phenomenological criteria such as Tsai-Hill, Maximum Stress and Maximum strain criteria. Fig 10 shows failure envelopes in the $\sigma_1 - \sigma_2$ plane for hybrid composite, with equal proportion of carbon and glass, respectively.

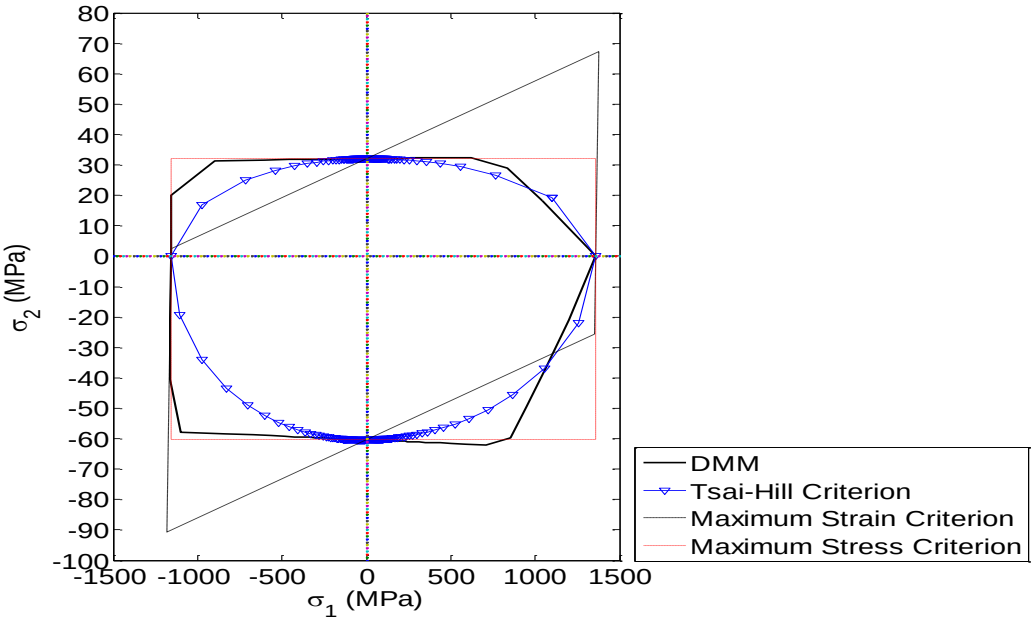

Fig 10. Failure Envelope for hybrid composite (30% carbon+30% glass) in σ_1- σ_2 plane

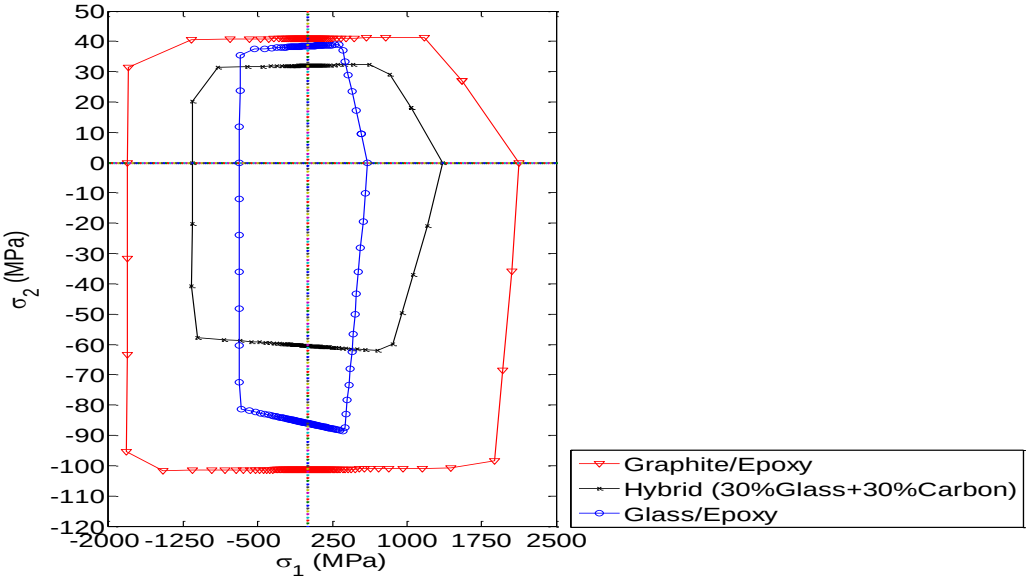

Fig 11. Relative comparison of DMM failure envelopes for composites in σ_1- σ_2 plane

As is evident from the above Fig 10, not one phenomenological criterion can effectively predict the strength of the composite. Since, the failure of the composite is generally matrix controlled for the longitudinal compressive and transverse compressive stresses, maximum stress theory shows a good match with DMM for these stresses. Tsai-Hill failure theory being a quadratic failure theory shows good match when failure is fiber controlled such as in the first quadrant, but under predicts the strength for all other cases. Similar is the case for maximum strain

theory, which over predicts the strength for the first and third quadrants while offers a conservative prediction for the second and fourth quadrant.

The failure envelope for the hybrid composite was compared with that for carbon/epoxy and glass/epoxy as shown in Fig 11. The longitudinal strength is a weighted mean of the volume of reinforcements as it follows the rule of mixtures. As for the transverse strength is considered, hybrid composites are very sensitive to the location of the fibers in the RVE. Variations of transverse tensile and compressive strengths are shown for the 10 samples analyzed are shown with respect to the changes in volume fraction in Fig 12 and 13, respectively. One way to accurately predict the variation in transverse strengths is to use statistical methods that can take into account the randomness in fiber locations and make a probabilistic prediction of the transverse strength or to come up with a RVE model that can capture the fiber randomness more effectively.

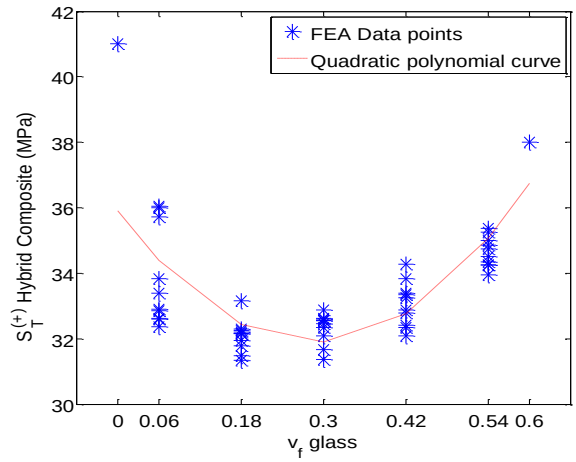

Fig 12. Variability in transverse tensile strength of hybrid composites as a function of glass fiber volume fraction

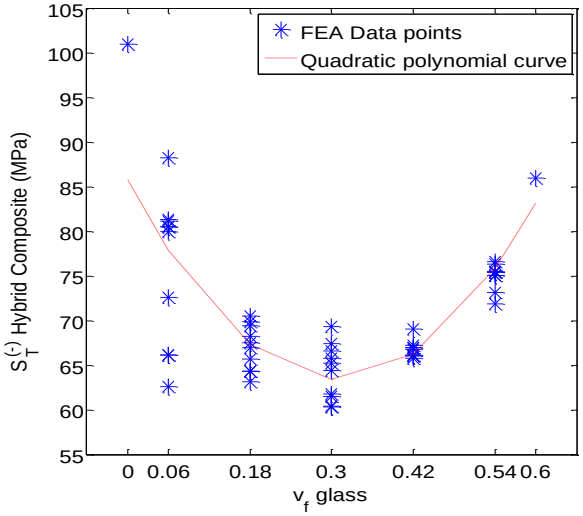

Fig 13. Variabiity in transverse compressive strength of hybrid composites as a function of glass fiber volume fraction

CONCLUSION

A computational model for hybrid composites using circular fibers in a hexagonal array has been proposed. Some of the parameters that play a key role in studying the hybrid effect on the stiffness and strength properties have been incorporated. The stiffness properties show a smooth linear variation with the change in volume fraction. Also orientation of the fibers in the unit cell did not affect the stiffness properties by and large. The reason for this behavior might be because of the fact that stiffness being a volume averaged quantity, doesn't depend on the position of the fibers but the overall effective volume fraction of the reinforcement only. The accuracy of the model was put to test by comparing results obtained from existing empirical and semi empirical relations. They showed a good match within limits of computational error.

Strength properties were also evaluated using Direct Micromechanics method and variation with volume fraction was also studied. Longitudinal tensile strength like the longitudinal modulus largely depends on the volume fraction of reinforcement and follows a linear trend. Although, longitudinal compressive strength was evaluated using similar methods, the accuracy of the data is still questionable. This is because, phenomena like micro-buckling and instability of fibers which largely govern the compressive strength, have not been taken into account.

Transverse strength for the composites has also been evaluated. It was observed that, transverse strength is highly sensitive to the location of the fibers inside the RVE. Use of statistical methods or a model that can better randomize the position and size of the fibers, which might better predict the transverse strength, remains a future work.

Overall, the idea of the present work was to come up with a design that is flexible enough to analyze a hybrid composite with any volume fraction and any reinforcement for variation in the properties. This might serve the designer looking for effective moduli of a composite with two or more fibers and give an estimate of failure initiation. Future work in this area would be to study such similar models and possibly formulate a closed form solution for predicting strength of any hybrid composite, without performing the finite element analysis.

ACKNOWLEDGEMENTS

The authors sincerely acknowledge the partial support of United States Army Research Office grant W911NF-08-1-0120 and encouragement of Dr. C.F. Yen of ARL at APG, MD.

REFERENCES

1. Chamis, C. C., Lark, R. F.,"Hybrid composites – State-of-the-art review: Analysis, Design, Application and Fabrication", NASA Technical Memorandum, NASA, TM X-73545
2. Chou, Tsu-Wei, Kelly, Anthony, "Mechanical properties of composites." Annu. Rev. Mater. Sci. 1980. 10:229-59
3. Fu S.-Y., Xu G., Mai Y.-W., "On the elastic modulus of hybrid particle/short-fiber polymer composites", Compos. Part B- Eng., 33, 291- 299, 2002.
4. Mirbagheri, Jamal, Tajvidi, Mehdi, Ghasemi, Ismaeil, Hermanson, John C., "Prediction of the Elastic Modulus of Wood Flour/Kenaf Fibre/Polypropylene Hybrid Composites", Iranian Polymer Journal, 16(4), 2007, 271-278
5. Chou, T. W. 1980 "Mechanical behavior of hybrid composites", Emerging Technologies in Aerospace Structures, Structural Dynamics and Materials, ed. J. R. Vinson, New York: American Society of Mechanical Engineers
6. Gibson, Ronald. F., "Principles of Composite Material Mechanics", Third Edition, CRC Press
7. Fu, Shao-Yun, Lauke Bernd, Mader, Hu Xiao, Yue Chee-Yoon, Mai Yiu-Wing, "Hybrid Effects on tensile properties of hybrid short-glass-fiber-and short-carbon-fiber- reinforced polypropylene composites", Journal of Materials Science 36 (2001) 1243-1251
8. Zhu, H., Sankar, B. V., Marrey, R. V., "Evaluation of Failure Criteria for Fiber Composites using Finite Element Micromechanics", Journal of Composite Materials, Vol 32, No. 8/1998
9. Choi, Sukjoo, Sankar, B. V., "Micromechanical Analysis of Composite Laminates at Cryogenic Temperatures", Journal of Composite Materials, Vol. 00, No. 00/2005
10. Hashin, Z., "Failure Criteria for Unidirectional Fiber Composites", Journal of Applied Mechanics, June 1980, Vol. 47
11. Stamblewski, Christopher, Sankar, B. V., Zenkert, Dan, "Analysis of Three-Dimensional Quadratic Failure Criteria for Thick Composites using the Direct Micromechanics Method", Journal of Composite Materials, 2008; 42; 635
12. Adams, D. F. and Doner, D. R. 1967 "Transverse normal loading of a unidirectional composite", Journal of Composite Materials, 1, 152-164
13. Adams, D. F. and Doner, D. R. 1967 "Longitudinal shear loading of a unidirectional composite", Journal of Composite Materials, 1, 4-17